Impact of Variable Perpendicular Transport Coefficients in WEST Simulations Using SolEdge-HDG

Ivan Kudashev, Anna Medvedeva Glasser, Manuel Scotto D'abusco, Eric Serre

Impact of variable perpendicular transport coefficients in WEST simulations using SolEdge-HDG

Ivan Kudashev, Anna Medvedeva Glasser, Manuel Scotto d' Abusco, Eric Serre

***Abstract*—Plasma-wall interaction is one of the key research topics on the way to controlled fusion. To study the best operational designs with reduced heat and particle fluxes onto tokamak plasma facing components comprehensive plasma simulations are required. A recent implementation of a Hybridized Discontinuous Galerkin scheme into a new version of SolEdge code has the advantage of using magnetic equilibrum free mesh. This allows to conduct pioneering 2D transport simulations of a full discharge in the WEST tokamak. In this work we implemented plasma transport coefficients as functions of coordinate in the poloidal plane and neutral diffusion as a function of neutrals mean free path. Moreover, the perpendicular convection flux terms were added into the code. Using the new features, few test cases were investigated. The influence of non-constant transport coefficients on the simulated particle and heat fluxes onto the WEST tokamak plasma facing components are demonstrated.**

***Index Terms*—Plasma transport, plasma simulation, heat exhaust, particle exhaust, Hybridizable Discontinous Galerkin (HDG), SolEdge**

I. Introduction

SIMULATIONS of fusion plasmas are getting more important not only on the eve of the ITER operations [1]. A number of machines are about to be launched in the coming years, both in public sector like SMART [2], DTT [3], as well as private projects such as ST-80, SPARC and ARC [4], [5]. Since such facilities will be used as testbeds for fusion energy production, which outcome strongly depends on the core plasma density, temperature and confinement time, the prediction of core plasma parameters is of great importance. However, part of the stored power will be still deposited on the wall while the highest acceptable heat flux is limited by engineering constraints. Therefore, it is also crucial to predict Scrape-off-Layer (SOL) parameters, because it will help to estimate the heat and particle fluxes onto the Plasma Facing Components (PFCs). All in all, turbulent transport in the whole plasma domain should be modeled with high level of confidence in order to allow safe and effective fusion facility operation.

This work has been supported by the French National Research Agency grant SISTEM (ANR-19-CE46-0005-03). This work has been carried out within the framework of the EUROfusion Consortium, funded by the European Union via the Euroatom Research and Training Programme (Grant Agreement No 101052200-EUROfusion). Views and opinions expressed are however those of the authors only and do not necessarily reflect those of the European Union or the European Commission. Neither the European Union nor the European Commission can be held responsible for them. Centre de Calcul Intensif d'Aix-Marseille is acknowledged for granting access to its high-performance computing resources.

Manuscript submitted October 03, 2023

One of the high-fidelity simulation tools chosen to simulate the whole plasma domain in ITER is JINTRAC [6] which employs coupling of core and edge codes. Though this approach is preferential due to detailed physics description in both confined and non-confined regions, one of the problems arises from the interface. Core codes are usually 1D assuming averaging over plasma surfaces while edge ones are 2D employing only toroidal symmetry. This difference requires cumbersome mapping between the two regions. Also, running in iterative way to reach self-consistency is time consuming. Another issue arises from the fact that 2D edge codes like SOLPS-ITER [7] or SOLEDGE-EIRENE [8] rely on magnetic field align meshes. This limits possibility to describe precisely plasma around PFCs. Moreover, if magnetic equilibrium changes, the whole mesh should be redefined. This results only in few configurations simulated, usually for flat-top phase of the discharge. On top of that, singularities occur in the vicinity of X-point and at the $\rho = 0$. First leads to cumbersome description of the domain near X-point, whereas the center region of plasma is usually omitted in the simulations.

Our group develops a new version of SolEdge code [9] based on Hybridizable Discontinuous Galerkin (HDG) scheme in order to solve previously discussed problems: necessity of coupling of different regions, being bounded to given magnetic equilibrium and cumbersome description of the domain boundary. The developed tool has the advantage of using high-order unstructured, non-aligned meshes. This allows modelling the whole plasma domain from PFCs to the very center of plasma. Releasing the mesh dependence on magnetic field topology leaded to full WEST discharge simulation from ramp-up to ramp-down [10]. This study demonstrated that SolEdge-HDG results decently follows the trends of the interferometer diagnostics. Also, it revealed the difference between steady and time evolving simulation approach, showing that the limiter phase might be crucial in predicting the global particle and impurity content of the plasma, which is not usually taken into account in typical stationary 2D simulations of the flat-top phase.

Despite of the remarkable results obtained with previous version of SolEdge-HDG [10], a main weakness of the model is to consider constant scalar perpendicular diffusion in the whole domain. This drawback significantly restricts the predictive capability of the code. Indeed, divertor fluxes depend strongly on SOL width which is closely related to perpendicular diffusion values near separatrix. Also, it is known that turbulent transport may vary with poloidal angle, for example,

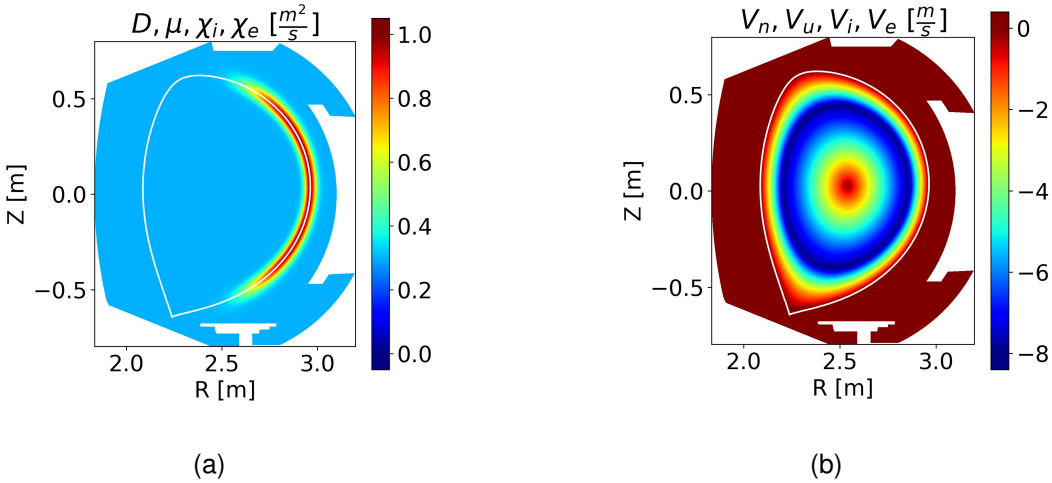

Fig. 1. 2D poloidal maps of (a) low field side ballooned diffusion ("ballooned" case) and (b) inward pinch velocities ("pinch" case) used in transport simulations in order to test new implemented features of SolEdge-HDG code. Separatrix postion is drown as a white line

in the case of ballooned interchange instability [11]. In [17] we have recently proposed an advanced modelling to self-consistently determine these perpendicular transport coefficients using additional characteristic variables of turbulence, k and epsilon. As a first step, we have enriched description of 2D transport by introducing coefficient maps as a function of coordinates in poloidal plane as a first step toward a richer physical model. Besides, the diffusion coefficient in the neutral continuity equation is now calculated based on mean free path, inspired by [14]. Moreover, the perpendicular convection flux terms were added, giving possibility to simulate anomalous or neoclassical pinch. The influence of non-constant transport coefficients on the simulated particle and heat fluxes are shown on three test cases.

The reminder of the paper is organized as follows. In section II the updated system of equation of SolEdge-HDG code is shown, as well as the simulation setup. Section III is dedicated to a discussion on the influence of applying different transport coefficients maps onto the midplane plasma density and temperature profiles as well as on heat and particle fluxes onto divertor targets. We draw out a conclusion in section IV with discussion on possible extents of this work.

II. SolEdge-HDG description and simulation parameters

SolEdge-HDG code solves 2D reduced Braginskii conservative equations for a deuterium plasma coupled with simplified neutral fluid model using Hybridizable Discontinuous Galerkin method. More details and assumptions can be found in [9] as well as in [10]. The updated equations with implemented perpendicular convection flux terms solved by SolEdge-HDG includes continuity equation:

$$\partial_t n + \nabla \cdot (nu\mathbf{b}) - \nabla \cdot (D\nabla_\perp n - V_n n\mathbf{b}_\perp) = S_n, \quad (1)$$

with quasineutrality assumed ($n = n_i = n_e$), $\mathbf{b}$ being the magnetic field unit vector, $\mathbf{b}_\perp$ unit vector perpendicular to magnetic field and the gradient being decomposed into $\boldsymbol{\nabla}_\parallel = \mathbf{b}\cdot\boldsymbol{\nabla}$ and $\boldsymbol{\nabla}_\perp = \boldsymbol{\nabla} - \mathbf{b}\cdot\boldsymbol{\nabla}_\parallel$. u is the parallel plasma velocity. D and V_n are perpendicular particle diffusion and pinch velocities respectively. S_n is a source term including ionization source and recombination sink and coupled with neutral continuity equation 5.

Second equation in the system is momentum conservation:

$$\partial_t(m_i nu) + \nabla \cdot (m_i nu^2\mathbf{b}) + \nabla_\parallel(k_b n(T_e + T_i)) - \nabla \cdot (\mu\nabla_\perp(m_i nu) - m_i nuV_u\mathbf{b}_\perp) = S_\Gamma, \quad (2)$$

with m_i being deuterium mass, T_i, T_e are the ion and electron temperatures respectively and k_b is the Boltzman constant. μ and V_u are viscosity and perpendicular momentum pinch velocity. S_Γ is momentum source due to plasma-neutral interaction.

Third and fourth equations are ion and electron energy conservation ones:

$$\partial_t\left(\frac{3}{2}k_b nT_i + \frac{1}{2}m_i nu^2\right) + \nabla \cdot \left(\left(\frac{5}{2}k_b T_i + \frac{1}{2}m_i nu^2\right)u\mathbf{b}\right) - nueE_\parallel - \nabla \cdot \left(\frac{3}{2}k_b(T_i D\nabla_\perp n + n\chi_i\nabla_\perp T_i) - \frac{3}{2}k_b T_i nV_i\mathbf{b}_\perp\right) - \nabla \cdot \left(-\frac{1}{2}m_i u^2 D\nabla_\perp n + \frac{1}{2}m_i\mu n\nabla_\perp u^2 - \frac{1}{2}m_i nu^2 V_u\mathbf{b}_\perp\right) - \nabla \cdot (k_{\parallel i}T_i^{\frac{5}{2}}\nabla_\parallel T_i\mathbf{b}) + \frac{3}{2}\frac{k_b n}{\tau_{ie}}(T_e - T_i) = S_{E_i}, \quad (3)$$

$$\partial_t\left(\frac{3}{2}k_b nT_e\right) + \nabla \cdot \left(\frac{5}{2}k_b T_e u\boldsymbol{b}\right) + nueE_\parallel - \nabla \cdot \left(\frac{3}{2}k_b(T_e D\nabla_\perp n + n\chi_e\nabla_\perp T_e) - \frac{3}{2}k_b T_e nV_e\mathbf{b}_\perp\right) - \nabla \cdot (k_{\parallel e}T_e^{\frac{5}{2}}\nabla_\parallel T_e\mathbf{b}) - \frac{3}{2}\frac{k_b n}{\tau_{ie}}(T_e - T_i) = S_{E_e}. \quad (4)$$

Neglecting inertia of electrons, the expression for the parallel electric field yields $enE_\parallel = -\nabla_\parallel(nk_b T_e)$. χ_i, χ_e and V_i,

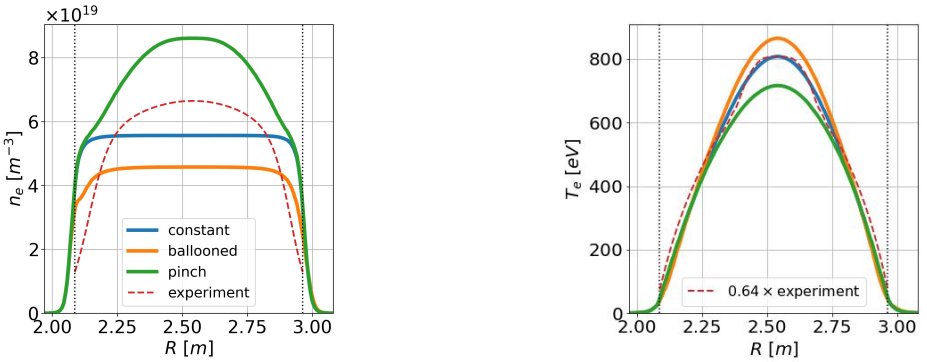

Fig. 2. SolEdge-HDG steady state simulation midplane profiles of electron (a) density and (b) temperature. Test cases with "ballooned" diffusion shown in figure 1a and inward "pinch" shown in figure 1b are compared with "constant" simulation with no pinch and constant diffusion. The experimental profiles plotted as dashed line (experimental electron temperature profile is rescaled to the maximum value of "constant" simulation). Dotted vertical lines represent separatrix location

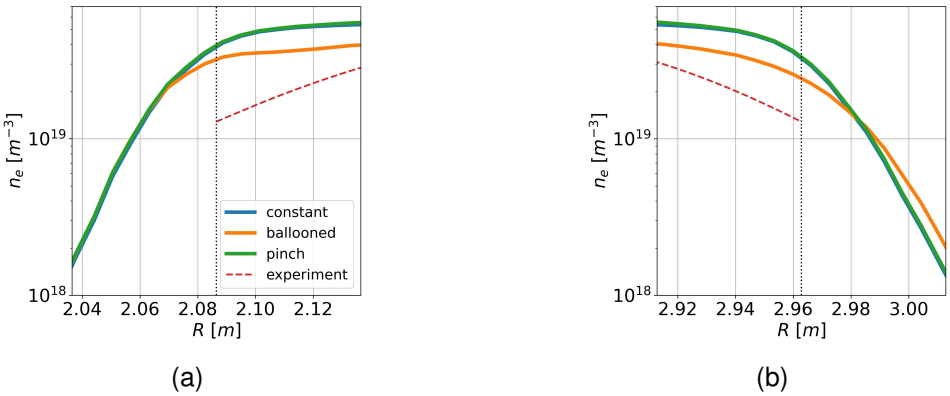

Fig. 3. Electron density profiles from figure 2a at the vicinity of (a) high field side and (b) low field side separatrix in logarithmic scale compared with experimental data (red dashed line). Dotted vertical lines represent separatrix location

V_e are the ion and electron perpendicular heat conductivity and pinch velocities. τ_{ie} is the relaxation time for energy exchange between ions and electrons. Parallel ion and electron heat conductivities for deuterium plasma are equal to $k_{\|i} = 60$ [$\mathrm{Wm^{-1}V^{-7/2}}$] and $k_{\|e} = 2000$ [$\mathrm{Wm^{-1}V^{-7/2}}$], defined according to [12]. S_e is electron energy source, which includes Ohmic heating and ad-hoc radiation losses. It is calculated employing Spitzer-Harm formulation of plasma resistivity [13] based on plasma current profile obtained from experimental data. S_i ion energy source, caused by interaction neutrals with plasma, with all Ohmic power is transfered to electrons as in the WEST experiment referent to this work. Perpendicular diffusion and pinch transport coefficients in the equations (1-4) can be prescribed as a 2D poloidal map. The fluid neutral equation is a simplified model from [14]:

$$\partial_t n_n - \nabla \cdot (D_{n_n} \nabla n_n) = S_{n_n,\mathrm{iz}} + S_{n_n,\mathrm{rec}} + S_{n_n}. \quad (5)$$

with n_n being neutrals density and neutral diffusion defined as:

$$D_{n_n} = \frac{eT_i[eV]}{m_i n(< \sigma v >_{\mathrm{cx}} + < \sigma v >_{\mathrm{iz}})}, \quad (6)$$

with upper bound of 20000 $\mathrm{m^2/s}$ to avoid numerical instabilities. We assume that neutrals have the same temperature as ions. $S_{n_n,\mathrm{iz}}$, $S_{n_n,\mathrm{rec}}$ are the ionisation and recombination sources coupled with continuity equation 1. S_{n_n} is neutral particle source defined by puff rate and recycling on the wall. Bohm conditions are aplied on the wall, same as in [10]. $< \sigma v_{\mathrm{iz}} >, < \sigma v_{\mathrm{rec}} >, < \sigma v_{\mathrm{cx}} >$ are ionisation, recombination and charge exchange rate coefficients based on ADAS [15] database. Ionisation and recombination rate coefficient implementation employs AMJUEL [16] splines on (t_e, n_e) grid.

Simulations, which are shown in this paper, are based on magnetic equilibrium and plasma current profiles of WEST discharge #54487 at t = 4.5s. We assume Z_{eff} = 1 in Ohmic heating source term. Recycling coefficient R = 0.95 in pump region and 0.99 elsewhere and puff rate of 7×10^{19} particles/s are chosen to approximately correspond to experimental density profiles.

Three test cases are considered and compared. "Constant" case is without pinch and with constant transport coefficients $D = \mu = \chi_i = \chi_e = 0.3$ $\mathrm{m^2/s}$, as implemented in the the previous version of the code. Second test case called

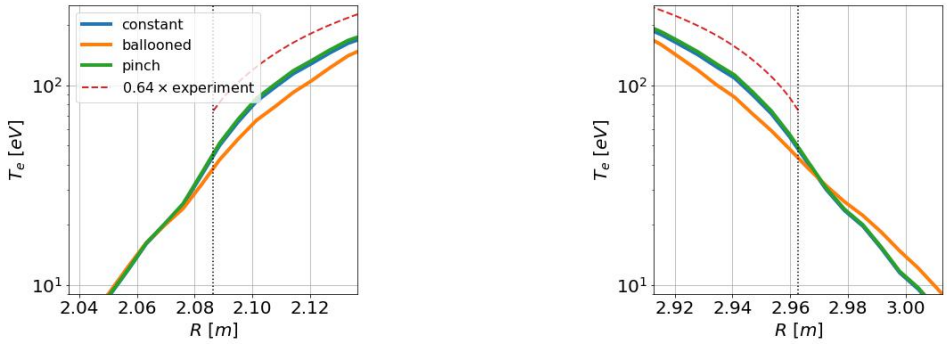

Fig. 4. Electron temperature profiles from figure 2b at the vicinity of (a) high field side and (b) low field side separatrix in logarithmic scale compared with rescaled experimental data (red dashed line). Dotted vertical lines represent separatrix location

"Ballooned" is addressed to model interchange instability, which is typical for tokamaks and leads to enhanced transport on the low field side (LFS) of the plasma domain in the vicinity of separatrix. The prescribed ballooned diffusion profile is defined by the expression

$$D = \mu = \chi_i = \chi_e = \ 0.3{+}0.7{\cdot}\exp(-(\frac{\rho-1}{0.05})^2-(\frac{\theta}{80})^8)\ \mathrm{m}^2/\mathrm{s} \tag{7}$$

is shown in figure 1a to approximately represent the results of [17]. ρ is the normalized poloidal flux coordinate (0 at magnetic axis, 1 at the separatrix), and θ is the poloidal angle mesured in degrees with $\theta = 0$ is on outer midplane (OMP). Third test case called "Pinch" relates to the fact that during previous simulations with SolEdge-HDG the resulting plasma density profiles were too flat in the core region comparing with experimental ones. This may be caused by the absence of perpendicular pinch in the original model, whereas clear evidences of turbulent and neoclassical pinch are present in the experiments and are predicted by theoretical studies [18]. Therefore an *ad-hoc* inward pinch has been imposed on all of the problem variables with $V_n = V_u = V_i = V_e = V_{pinch}(\rho)$. It is shown in figure 1b and defined by an analytical expression for

$$V_{pinch} = \begin{cases} -10\rho \text{ m/s}, \rho \leq 0.8 \\ -40 \cdot (1-\rho) \text{ m/s}, 0.8 < \rho \leq 1.0 \\ 0, \rho > 1.0 \end{cases} \tag{8}$$

Diffusion transport coefficients are left the same as in the "constant" case.

III. Simulation results

In this section we compare the results of these 3 cases: with constant diffusion and no pinch ("Constant"), with ballooned diffusion 1a and no pinch ("Ballooned") and with pinch 1b and constant diffusion ("Pinch"). We will focus our anylysis on midplane and divertor profiles.

The midplane profiles are shown in figure 2. Enlarged data representation at the vicinity of the low and high field side (HFS) separatrix is introduced in figure 3 and 4. From the figures we can clearly see the influence of the imposed transport coefficients. Increased ballooned perpendicular transport reduces global particle content which leads to a simultaneous slight increase of central temperature. As expected, in "ballooned" case only low field side of scrape-off layer is significantly altered. At the same time, imposed only in the core region, pinch has almost negligible impact in the SOL on both temperature and density profiles. Despite the fact that inward pinch has been imposed on all plasma variables, change in perpendicular transport had primary effect on density, which results in its peaking. Hence, having almost the same Ohmic heating, defined by plasma current, simulated electron temperature decreased.

Further we compare simulation midplane density and temperature profiles with the experimental ones. From the figure 2a we can see that density shape is better reproduced by the "pinch" case. This means that for interpretive simulations one should have inward pinch imposed in the core region. Herewith, separatrix density is significantly higher than experimental one, therefore, higher diffusion or outward pinch should be applied in the edge region. However, one should carefully consider experimental density profiles since they are routinely obtained by inversion of limited amount of interferometer lines of sight with prescribed shape of hyperbolic tangent. Another reason for the very high density at the separatrix and a relatively flat profile in the core could be attributed to the plasma density source location resulting from neutrals ionization. It seems that for such a high density almost all neutrals are ionized before crossing the separatrix. This first leads to the overestimated density at the vicinity of the LCFS and also to the lack of a source in the core plasma, which results in very flat density profiles. However, an in-depth investigation of the ionization source location is part of an upcoming study and falls beyond the scope of this paper. At this point, we can only suggest that introducing higher-Z impurities into the model, which are harder ionized in the SOL, may add particle sources in the confined plasma leading to more bell-like density profiles.

Opposite to density, we can see systematic temperature underestimation for the considered test cases (figure 2b). The

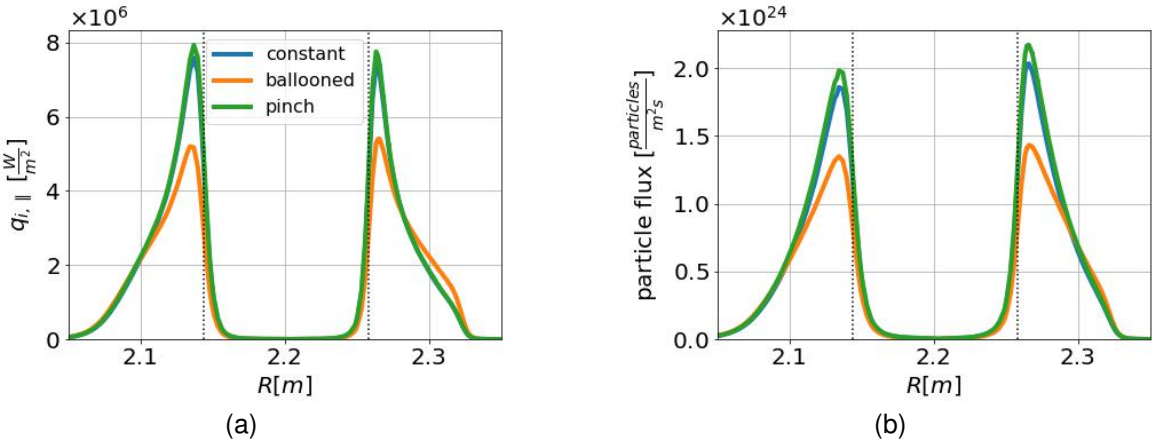

Fig. 5. SolEdge-HDG test case steady state simulations divertor profiles of (a) parallel ion heat and (b) particle fluxes onto divertor targets. Test cases with "ballooned" diffusion shown in figure 1a and inward "pinch" shown in figure 1b are compared with "constant" simulation with no pinch and constant diffusion. Strike points are shown as dotted lines

main reason for this discrepancy lies in the assumed Z_{eff} = 1, when in the experiment values higher than 2 can be easily observed. Therefore, we focus more on the shape of the temperature profiles rather than on the value. According to that we have rescaled the experimental T_e profile to the maximum value of "constant" test case. We can see now that simulated temperature profiles almost repeat the experimental one in shape. However, closer to separatrix the modeled values decay faster. This can be possibly corrected by choosing similar transport coefficients which will reduce edge density in the simulation, leading to increase temperature since the Ohmic heating power will remain mostly unchanged.

Another region of interest is the divertor targets, since in fusion devices most of the power will be deposited there. No experimental data is available for target profiles for this shot, so only simulated data is considered. Parallel ion energy and particle fluxes are shown on figure 5 with R being major radius of the tokamak. Pinch applied inside the separatrix doesn't change perpendicular transport in the SOL, hence, there are no significant changes of the profiles in the non-confined region compared with the "constant" case. A slight increase of peak fluxes values correspond to the increase of global particle content seen in figure 2a. On the contrary, ballooned diffusion notably reduces peak values of both particle and heat fluxes due to increased perpendicular transport. Moreover, its ballooned nature results in a shoulder in the vicinity of the outer strike point. In order to quantitatively study the difference in the fluxes width, target decay lengths of both particle and heat fluxes have been calculated by fitting simulated data to the Eich's formula [19]:

$$q(\overline{s}) = \frac{q_0}{2}\exp\left(\left(\frac{S}{2\lambda_{q,n}}\right)^2 - \frac{\overline{s}}{\lambda_{q,n}}\right)\cdot\mathrm{erfc}\left(\frac{S}{2\lambda_{q,n}} - \frac{\overline{s}}{S}\right) - q_{\mathrm{BG}}, \tag{9}$$

with q being the heat or particle flux, $\overline{s}$ is the distance from the corresponding strike point along the target, $\lambda_{q,n}$ is heat or particle flux decay length, q_0, q_{BG} are the peak and background values of the flux, S is the width of the Gaussian describing diffusive transport into private flux region. λ_q, q_0, q_{BG}, S are free fitting parameters. The calculated heat and particle flux decay length for both HFS and LFS are introduced in tables I, II respectively. We can clearly see that imposing ballooned diffusion increases both LFS and HFS decay lengths by approximately 25%. In future work ballooned transport will be self-consistently simulated with model from [17] and it will be possible to study its influence on the fluxes on the targets and their widths.

TABLE I
PARALLEL HEAT FLUX DECAY LENGTH

case label	$\lambda_{q,\parallel,hfs}$ [mm]	$\lambda_{q,\parallel,lfs}$ [mm]
constant	18	17
ballooned	23	23
pinch	18	17

TABLE II
PARALLEL PARTICLE FLUX DECAY LENGTH

case label	$\lambda_{n,\parallel,hfs}$ [mm]	$\lambda_{n,\parallel,lfs}$ [mm]
constant	19	18
ballooned	22	22
pinch	19	18

Introduced test cases demonstrate that numerically the SolEdge-HDG code can handle new upgrades of the perpendicular transport terms and give reasonable solutions depending on the set of imposed transport coefficients. The code now is reaching enough flexibility to be used like an interpretive tool. Furthermore, it will be easier to couple SolEdge-HDG with other codes like QuaLiKiz [20] , NCLASS [21] or employ models like in [17] to get physically reliable values of turbulent and neoclassical transport coefficients. With these updates SolEdge-HDG may become a powerful predictive tool.

IV. CONCLUSION

In this contribution we have introduced the recent updates of the physical model encompassed into system of equations of the SolEdge-HDG code. Having these modifications it is now

possible to describe diffusion coefficients as 2D poloidal maps. Also perpendicular convection terms can now be described via SolEdge-HDG. In addition, the neutral continuity equation has been improved, calculating diffusion coefficient based on neutrals mean free path.

To demonstrate the new capabilities of the code three test cases have been compared, a ”constant” with no pinch and constant diffusion, a ”ballooned” with no pinch and ballooned on a low field side separatrix diffusion and ”pinch” with an inward pinch and constant diffusion. As expected, ballooned diffusion flattens temperature and density profiles at the vicinity of the separatrix as well as widens fluxes onto the divertor. Besides, pinch imposed in the confined region increases the core density peaking with almost no change outside of the separatrix.

With features demonstrated in this work the SolEdge-HDG is already a much more flexible in interpretive modeling. In further studies time advancing simulation of the whole discharge with self-consistently defined turbulent perpendicular transport will be conducted. Also, other ways to describe the transport coefficients will be tested, like analytical expressions or coupling with other codes such as QuaLiKiz or NCLASS, in order to increase predcitve power of SolEdge-HDG. Having both SOL and confined plasma described by one code will allow to study interaction between different core and edge models.

ACKNOWLEDGMENTS

Centre de Calcul Intensif d'Aix-Marseille is acknowledged for granting access to its high-performance computing resources.

REFERENCES

[1] B. Bigot, “ITER construction and manufacturing progress toward first plasma,” *Fusion Eng. Des.*, 146, pp.124-129, 2019.
[2] A. Mancini, et al. “Predictive simulations for plasma scenarios in the SMART tokamak,” *Fusion Eng. Des.*, 192, 113833, 2023.
[3] R. Ambrosino “DTT-Divertor Tokamak Test facility: A testbed for DEMO,” *Fusion Eng. Des.*, 167, 112330, 2021.
[4] S. Meschini “Review of commercial nuclear fusion projects,” *Front. Energy Res.*, 11, 1157394, 2023.
[5] *Fusion Industry Association*. [Online]. Available: https://www.fusionindustryassociation.org/.
[6] M. Romanelli, et al. “JINTRAC: a system of codes for integrated simulation of tokamak scenarios,” in *Plasma Fusion Res.*, 9, pp.3403023-3403023, 2014.
[7] S. Wiesen, et al. “The new SOLPS-ITER code package,” in *J. Nucl. Mater.*, 463, 480-484, 2015.
[8] H. Bufferand, et al. “Three-dimensional modelling of edge multi-component plasma taking into account realistic wall geometry.” *Nucl. Mater. Energy* 18 (2019): 82-86. S. Wiesen, et al. “The new SOLPS-ITER code package,” in *J. Nucl. Mater.*, 463, 480-484, 2015.
[9] G. Giorgiani, et al. “A hybrid discontinuous Galerkin method for tokamak edge plasma simulations in global realistic geometry,” *J. Comput. Phys.*, 374, pp.515-532, 2018.
[10] M.S. d' Abusco, et al. “Core-edge 2D fluid modeling of full tokamak discharge with varying magnetic equilibrium: from WEST start-up to ramp-down,” *Nucl. Fusion*, 62(8), p.086002, 2022.
[11] N. Fedorszak “Experimental investigation of turbulent transport at the edge of a tokamak plasma,”, PhD thesis, 2010.
[12] P. C. Stangeby “The plasma boundary of magnetic fusion devices,”, Philadelphia, Pennsylvania: Institute of Physics Pub,Vol. 224, 2000.
[13] J. Wesson and D.J. Campbell. “Tokamaks,” International Series of Monogr. OUP Oxford, 2011
[14] N. Horsten, et al. “Development and assessment of 2D fluid neutral models that include atomic databases and a microscopic reflection model,” *Nucl. Fusion*, 57.11, 116043, 2017.
[15] H. Summers. The ADAS user manual, version 2.6. [Online]. Available: http://www. adas. ac. uk/ 2004
[16] D. Reiter. The data file AMJUEL: additional atomic and molecular data for EIRENE. in *Technical Report FZ Juelich*, 2000
[17] S. Baschetti, et al. “Self-consistent cross-field transport model for core and edge plasma transport,” *Nucl. Fusion*, 61(10), p.106020, 2021.
[18] C. Angioni, et al. “Particle transport in tokamak plasmas, theory and experiment,” *Plasma Phys. Control. Fusion*, 51.12, 124017, 2009.
[19] T. Eich, et al. “Inter-ELM power decay length for JET and ASDEX upgrade: measurement and comparison with heuristic drift-based model,” *Phys. Rev. Lett.*, 107(21), 215001, 2011.
[20] J. Citrin, et al. “Tractable flux-driven temperature, density, and rotation profile evolution with the quasilinear gyrokinetic transport model QuaLiKiz,” *Plasma Phys. Control. Fusion*, 59.12, 124005, 2017.
[21] W. A. Houlberg, et al. “Bootstrap current and neoclassical transport in tokamaks of arbitrary collisionality and aspect ratio,” *Phys. Plasmas*, 4.9, 3230-3242, 1997.